AD-763 716

EFFECT OF H2 PRESSURE ON PULSED H2+F2 LASER, EXPERIMENT AND THEORY

Steven N. Suchard, et al

Aerospace Corporation
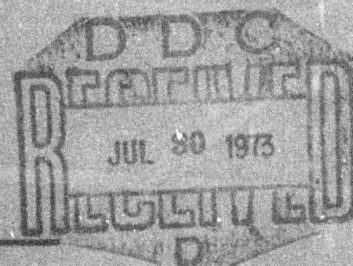
Prepared for:

Space and Missile Systems Organization

30 March 1973

AD 763716

Effect of H_2 Pressure on Pulsed $H_2 + F_2$ Laser, Experiments and Theory

Prepared by
MECHANICS RESEARCH and CHEMICAL KINETICS DEPARTMENTS
Aerophysics Laboratory

73 MAR 30

D D C
JUL 30 1973

Laboratory Operations
THE AEROSPACE CORPORATION

Prepared for SPACE AND MISSILE SYSTEMS ORGANIZATION
AIR FORCE SYSTEMS COMMAND
LOS ANGELES AIR FORCE STATION
Los Angeles, California

APPROVED FOR PUBLIC RELEASE:
DISTRIBUTION UNLIMITED

LABORATORY OPERATIONS

The Laboratory Operations of The Aerospace Corporation is conducting experimental and theoretical investigations necessary for the evaluation and application of scientific advances to new military concepts and systems. Versatility and flexibility have been developed to a high degree by the laboratory personnel in dealing with the many problems encountered in the nation's rapidly developing space and missile systems. Expertise in the latest scientific developments is vital to the accomplishment of tasks related to these problems. The laboratories that contribute to this research are:

Aerophysics Laboratory: Launch and reentry aerodynamics, heat transfer, reentry physics, chemical kinetics, structural mechanics, flight dynamics, atmospheric pollution, and high-power gas lasers.

Chemistry and Physics Laboratory: Atmospheric reactions and atmospheric optics, chemical reactions in polluted atmospheres, chemical reactions of excited species in rocket plumes, chemical thermodynamics, plasma and laser-induced reactions, laser chemistry, propulsion chemistry, space vacuum and radiation effects on materials, lubrication and surface phenomena, photosensitive materials and sensors, high precision laser ranging, and the application of physics and chemistry to problems of law enforcement and biomedicine.

Electronics Research Laboratory: Electromagnetic theory, devices, and propagation phenomena, including plasma electromagnetics; quantum electronics, lasers, and electro-optics; communication sciences, applied electronics, semiconducting, superconducting, and crystal device physics, optical and acoustical imaging; atmospheric pollution; millimeter wave and far-infrared technology.

Materials Sciences Laboratory: Development of new materials; metal matrix composites and new forms of carbon; test and evaluation of graphite and ceramics in reentry; spacecraft materials and electronic components in nuclear weapons environment; application of fracture mechanics to stress corrosion and fatigue-induced fractures in structural metals.

Space Physics Laboratory: Atmospheric and ionospheric physics, radiation from the atmosphere, density and composition of the atmosphere, aurorae and airglow; magnetospheric physics, cosmic rays, generation and propagation of plasma waves in the magnetosphere; solar physics, studies of solar magnetic fields; space astronomy, x-ray astronomy; the effects of nuclear explosions, magnetic storms, and solar activity on the earth's atmosphere, ionosphere, and magnetosphere; the effects of optical, electromagnetic, and particulate radiations in space on space systems.

THE AEROSPACE CORPORATION
El Segundo, California

DOCUMENT CONTROL DATA - R & D

(Security classification of title, body of abstract and indexing annotation must be entered when the overall report is classified)

1. ORIGINATING ACTIVITY *(Corporate author)*	2a. REPORT SECURITY CLASSIFICATION
The Aerospace Corporation El Segundo, California	Unclassified
	2b. GROUP

3. REPORT TITLE

EFFECT OF H₂ PRESSURE ON PULSED H₂ + F₂ LASER, EXPERIMENT AND THEORY

4. DESCRIPTIVE NOTES *(Type of report and inclusive dates)*

5. AUTHOR(S) *(First name, middle initial, last name)*

Steven N. Suchard, Ronald L. Kerber, George Emanuel, and James S. Whittier

6. REPORT DATE	7a. TOTAL NO. OF PAGES	7b. NO. OF REFS
73 MAR 30	49	40

8a. CONTRACT OR GRANT NO.	9a. ORIGINATOR'S REPORT NUMBER(S)
F04701-72-C-0073	TR-0073(3540)-1
b. PROJECT NO.	
c.	9b. OTHER REPORT NO(S) *(Any other numbers that may be assigned this report)*
d.	SAMSO-TR-73-207

10. DISTRIBUTION STATEMENT

Approved for public release; distribution unlimited

11. SUPPLEMENTARY NOTES	12. SPONSORING MILITARY ACTIVITY
	Space and Missile Systems Organization Air Force Systems Command Los Angeles, California

13. ABSTRACT

Stimulated emission predictions and measurements for an $H_2 + F_2$ laser are compared for H_2 pressures from threshold to stoichiometric, a range of several orders of magnitude. Slowly flowing, helium-diluted, 50-Torr mixtures are initiated photolytically. Two dilution ratios and two output couplers are considered, and good agreement is found for time to threshold and pulse duration vs H_2 pressure. Spiking, relaxation oscillations, and possibly mode beating, features not modeled, are observable in some pulses; however, predicted intensity vs time generally agrees in pulse shape with laser output. Observed and predicted peak intensities nearly match for low H_2 pressure, and the predicted increase of peak intensity with low H_2 is followed fairly well. For H_2 in the vicinity of one-tenth stoichiometric, the peak intensity data show an abrupt leveling off, while the calculations predict a continuing increase. This disagreement most probably cannot be attributed to uncertainties in the kinetic model. All rate modifications considered have proven incapable of producing a change sufficiently large or abrupt to explain this feature of the data. Experimental results are presented supporting the notion that parasitic oscillations cause this change in laser output.

14   **KEY WORDS**

Chain-reaction laser
Chemical laser
Chemical laser modeling
Hydrogen fluoride laser
Laser

Distribution Statement (Continued)

Abstract (Continued)

EFFECT OF H_2 PRESSURE ON PULSED H_2 + F_2 LASER, EXPERIMENT AND THEORY

Prepared by

MECHANICS RESEARCH and CHEMICAL KINETICS DEPARTMENTS
Aerophysics Laboratory

73 MAR 30

Laboratory Operations
THE AEROSPACE CORPORATION
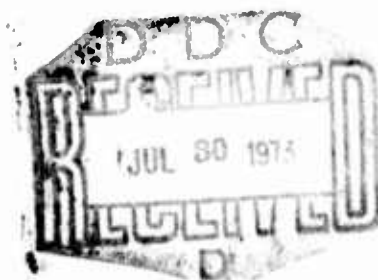
Prepared for

SPACE AND MISSILE SYSTEMS ORGANIZATION
AIR FORCE SYSTEMS COMMAND
LOS ANGELES AIR FORCE STATION
Los Angeles, California

ic

FOREWORD

This work reflects research supported by the Defense Advanced Research Projects Agency of the Department of Defense under U. S. Air Force Space and Missile Systems Organization (SAMSO) Contract No. F04701-72-C-0073.

This report was prepared by S. N. Suchard, R. L. Kerber, and J. S. Whittier of the Mechanics Research Department and G. Emanuel of the Chemical Kinetics Department of the Aerophysics Laboratory.

The authors gratefully acknowledge the assistance of N. Cohen for his help with the kinetics, and A. Ching, L. D. Bergerson, J. F. Bott, M. A. Kwok, and J. S. Lesser for their assistance in various phases of this work.
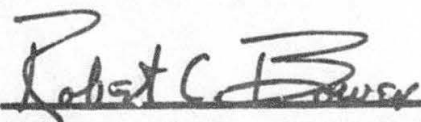
This work, which documents research carried out from September 1971 through February 1972, was submitted on 31 January 1973 for review and approval to Capt Robert C. Bower, DYX.

Approved

W. R. Warren, Jr., Director
Aerophysics Laboratory

Publication of this report does not constitute Air Force approval of the report's findings or conclusions. It is published only for the exchange and stimulation of ideas.

Robert C. Bower, Capt. USAF
Project Officer

ABSTRACT

Stimulated emission predictions and measurements for an $H_2 + F_2$ laser are compared for H_2 pressures from threshold to stoichiometric, a range of several orders of magnitude. Slowly flowing, helium-diluted, 50-Torr mixtures are initiated photolytically. Two dilution ratios and two output couplers are considered, and good agreement is found for time to threshold and pulse duration vs H_2 pressure. Spiking, relaxation oscillations, and possibly mode beating, features not modeled, are observable in some pulses; however, predicted intensity vs time generally agrees in pulse shape with laser output. Observed and predicted peak intensities nearly match for low H_2 pressure, and the predicted increase of peak intensity with low H_2 is followed fairly well. For H_2 in the vicinity of one-tenth stoichiometric, the peak intensity data show an abrupt leveling off, while the calculations predict a continuing increase. This disagreement most probably cannot be attributed to uncertainties in the kinetic model. All rate modifications considered have proven incapable of producing a change sufficiently large or abrupt to explain this feature of the data. Experimental results are presented supporting the notion that parasitic oscillations cause this change in laser output.

CONTENTS

FIGURES

TABLES

I. INTRODUCTION

Measurements and theoretical predictions of stimulated emission for an $H_2 + F_2$ laser are compared in this report over a wide range of initial H_2 concentrations. While such comparisons were heretofore unavailable, several earlier studies of pulsed $H_2 + F_2$ chemical lasers have been reported.[1-16] Experimental investigations have shown the existence of lasing for several mixtures and initiation methods, and have presented the laser's spectrum[1-3,5,16] or time-resolved spectrum.[7,8,12] Most of this work, however, gives very limited information about the effect on the laser pulse of changes in mixture composition. Notable exceptions are the works of Hess[11] and Dolgov-Savel'yev.[7] Hess investigated the effect of total pressure with a fixed composition ratio $H_2:F_2:He = 0.33:1:40$ and the effect of varying the H_2/F_2 ratio over a limited range. Hess also presents results of simplified rate equation calculations for the reacting mixture but without including the effect of stimulated emission. He finds that his experimental laser pulses terminate at times, for which his calculations indicate substantial completion of the reaction.

A previous work that gives calculations of stimulated emission for the $H_2 + F_2$ pulsed laser[17] contains no comparisons with experiment. It nevertheless identifies the relative importance of the mechanisms in the theory and shows the predicted effects of varying initial composition, temperature, and the optical cavity.

Pioneering comparisons of pulsed chemical laser experiments with theoretical calculations are given by Airey[18] for an HCl laser pumped by the reaction between hydrogen bromide and photolytically produced atomic chlorine. We extend Airey's approach to the more complicated $H_2 + F_2$ system where vibration-rotation bands cascade and where chain-reaction pumping can extend the laser pulse well beyond the duration of the flashlamp used for photolytic initiation. Moreover, the larger gain of HF as compared with HCl gives rise to experimental complications apparently not present in the work of Airey.

Emanuel and co-workers[19] formulated a multilevel chemical laser theory and computer simulation for prediction of laser performance from a rate model, thermodynamic and spectroscopic properties, and parameters describing the laser cavity. In addition, Cohen[20] gives a critical assessment of rate coefficients for reactions in the $H_2 + F_2$ laser system, along with a recommended set of "best" values for these rates. We incorporated the rate model suggested by Cohen* into the theoretical model and present the first comparison of pulsed $H_2 + F_2$ laser experiments with complementary theoretical predictions.

The experiments measure output intensity vs time as a function of the hydrogen-to-fluorine ratio. The reacting mixture has a fixed total pressure of 50 Torr with varying initial composition, and the H_2/F_2 mole ratio is varied from 0.0008 to 1 with the He/F_2 mole ratio at 20 or 40. Two different output coupling mirrors are used. Traces of HF in the reacting mixture before initiation are measured by determining the attenuation of a probe beam from a

---

*The rates used in our calculations reflect some new values obtained since the preparation of Ref. 20. Details are given in the Appendix.

line-selected HF laser. Our experiments are distinguished from earlier work by their detailed study over a wide range of initial hydrogen concentrations and by the measurement of initial HF concentrations, a precaution not included in previous work.

Experimental and predicted pulse shapes are qualitatively very similar. Measurements and predictions of time to laser threshold and pulse duration vs hydrogen partial pressure are in good agreement. For H_2/F_2 ratios less than 0.1, modeling and experimental results have the same trend in peak intensity vs hydrogen partial pressure. For H_2/F_2 ratios greater than 0.1, our calculations predict a continuing increase of peak intensity with increasing hydrogen; however, the experimental data for peak intensity in this region exhibit an abrupt leveling off. With $H_2/F_2 = 1.0$, the peak intensity is barely larger than at $H_2/F_2 = 0.1$. This behavior most probably cannot be attributed to uncertainties in the kinetic model. All rate modifications considered have proven to be incapable of introducing a sufficiently large or abrupt change in the peak intensity vs H_2 curve to explain the data. Supplementary experimental results are presented supporting the notion that parasitic oscillations are the cause for this decrease in laser output. This indicates that previous pulsed HF laser work may, in part, be misleading because of the presence of parasitic oscillations.

II. EXPERIMENTAL PROCEDURES

Experiments were performed with a flash photolysis laser apparatus.[12]
A quartz laser tube with a 1.27-cm i.d. and 55.3 cm in length was attached to
aluminum window holders machined to the Brewster angle for NaCl. The tube en-
closed a continually flowing reactant mixture. A laser cavity 100 cm in length
was formed by a spherical mirror of 8.8-m radius and a dielectric-coated flat
of either 25% transmittance (sapphire substrate) or 65% transmittance (silicon
substrate). The spherical mirror was gold-coated to a nominal reflectivity of
98%.

Helium (Matheson, 99.99%) and fluorine (Matheson, 98%) are premixed at a
mole ratio of 10 to 1 and a pressure of 7.1 atm in a passivated stainless steel
bottle having a perforated sting to ensure complete mixing. The remainder of
the gas sample, H_2 (Matheson, 99.998%), and additional He is flow monitored and
mixed with the F_2-He sample in an aluminum mixing block. The F_2-He mixture is
injected through a calibrated sonic orifice into the H_2-He flow. As a pre-
caution against preignition of the mixture,[21] tubing from the mixer to the
laser tube and from the laser tube to a carbon trap is of Teflon and aluminum.
The carbon trap protects the vacuum pump from unreacted F_2. Flame propagation
from the carbon trap back into the laser tube is discouraged by an aluminum
screen flame arrestor in this exhaust line. Gases from the laser tube are ex-
hausted by a 15 ft^3/min mechanical vacuum pump (Kinney KC-15). Pressures are
measured with gauges (Heise) having Cu-Be Bourdon tubes.

Preceding page blank

A 14.7 µF/20 kV capacitor (Sangamo), ignitron triggered, is discharged through a xenon flashlamp (Kemlite) with an active length of 56 cm to initiate the laser reaction. The lamp and laser tube are 5 cm apart and are optically coupled by a closely wrapped aluminum foil reflector. Flashlamp output is monitored by means of a 929 photodiode (RCA).

Laser radiation is monitored with a Au:Ge detector (Raytheon) placed 100 cm from the output coupling mirror. The sensitive area of the detector, which measures 2 mm in diameter, acts as an aperture so that only radiation very near the laser axis is monitored. Calibration against a black body source indicates that, for the wavelengths of interest, the detector has a sensitivity of 0.97 V/W with a 50-Ω load. Total risetime of the detector and oscilloscope is known from other experiments to be about 20 nsec.

Precise values for initial concentrations of the various reactants are desired. Therefore, we measure the extent of the prereaction between the H_2 and F_2 before flash initiation and the amount of HF initially present in the F_2. Two independent techniques are employed: the first measures the change in the fluorine concentration as H_2 is introduced, and the second measures the HF pressure in the reactants prior to photolysis.

In the first method, uv radiation from a high pressure dc mercury lamp is split into two beams; one beam passes through the laser where it is partially absorbed by the F_2, while the other is used as a reference. By means of a mechanical chopper, the beams are displayed alternately to a photomultiplier covered by a band filter, 290 $\pm$ 10 nm, centered near the F_2 absorption peak.[22]

The photomultiplier output (square wave) is displayed on an oscilloscope and is interpreted by a differencing procedure.[23] With this technique, we are able to measure changes of a few percent in the F_2 partial pressure. Under the conditions of the present experiments, the F_2 partial pressure was found to remain constant, independent of the H_2 partial pressure.

The second method uses infrared absorption to measure directly the HF(0) concentration in the laser tube. A transverse electrical discharge HF laser[24] is used for this purpose. In this laser, ninety 100-Ω resistors in parallel act as pin electrodes for discharge of a 1500-pF capacitor charged to 15 kV through an H_2 + SF_6 mixture (mole ratio 1 to 10) at a total pressure of 50 Torr. The optical cavity consists of a spherical mirror with a 3.15-m radius of curvature and a 2-mm hole for output coupling, gold-coated to a nominal reflectivity of 98%, and a plane reflectance grating (PTR) with 7200 lines/in. blazed at 2.6 μm. With this arrangement, individual transitions in the v = 3→2, 2→1, or 1→0 bands could be selected. The present measurements used the $P_1(3)$, $P_1(5)$, and $P_1(7)$ transitions.

Absorption coefficients associated with each of these laser lines are determined, in place, by measuring the attenuation of each line with a known pressure of HF(0) in the laser tube. A dual-beam experiment is used to avoid error because of variability of the line-selected laser's pulse amplitude (typically $\pm 15\%$). The line-selected laser beam is split with a reference beam sent directly to a detector and a probe beam sent through the photolysis laser tube before detection. Nominally identical Au:Ge (Raytheon) detectors are used for the two beams. The attenuation of the probe beam is calculated from

-7-

measurements of the ratio of the probe to the reference beam with and without HF(0) in the laser tube. Values determined for absorption coefficients of the probe transitions are: $K_0[P_1(3)] = 6.50 \pm 0.21(cm\text{-}Torr)^{-1}$, $K_0[P_1(5)] = 1.92 \pm 0.18(cm\text{-}Torr)^{-1}$, and $K_0[P_1(7)] = 0.27 \pm 0.02(cm\text{-}Torr)^{-1}$.

After calibration, the dual-beam laser absorption apparatus is used to determine the amount of HF(0) present in the F_2 or in the H_2-F_2-He mixtures before initiation. As shown in Fig. 1, the F_2 sample contained approximately 1.6 ± 0.3 mTorr of HF(0) per Torr of F_2. In addition, trace amounts of pre-reaction of $H_2 + F_2$ are indicated by the rising portions of the curves in Fig. 1.
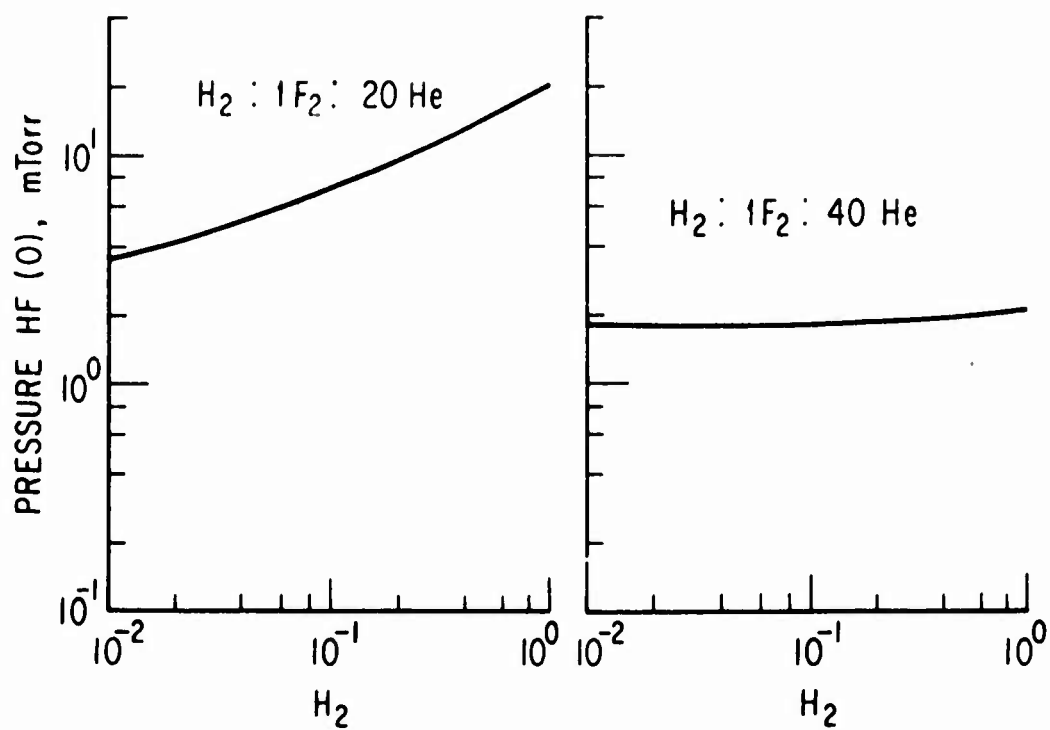
Fig. 1. Trace Concentrations of HF in Various $H_2:F_2:$He Mixtures Before Flash Initiation

III. COMPUTER SIMULATION

The chemical laser computer simulation used is described in Ref. 19, but a resumé of its features is presented in this section. Rate equations are used to represent the chemical kinetic and stimulated emission processes occurring in a representative unit volume within a Fabry-Perot cavity. All processes are assumed uniform throughout the cavity. Rotational equilibrium at the translational temperature T is assumed. Only the transition with maximum gain in each band is assumed to lase; this is always in the P-branch. Combined Doppler and collisional broadening (Voigt profile) is modeled. During lasing, the gain at line center is held constant at the threshold value for the cavity; the gain profile is assumed to saturate homogeneously.

Reaction of the H_2 + F_2 + diluent mixture is represented by:

1. Photodissociation of F_2

$$F_2 + h\nu \longrightarrow 2F$$

2. The H_2 - F_2 chain

$$F + H_2 \rightleftharpoons HF(v) + H$$

$$H + F_2 \rightleftharpoons HF(v) + F$$
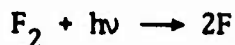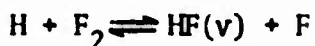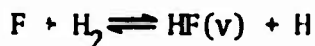
3. Vibrational-translational (VT) deactivation

$$HF(v) + M \rightleftharpoons HF(v-1) + M$$

$$H_2(v) + M \rightleftharpoons H_2(v-1) + M$$

4. Vibrational-vibrational (VV) quantum exchange

$$HF(v) + HF(v') \rightleftharpoons HF(v+1) + HF(v'-1)$$

$$HF(v) + H_2(v') \rightleftharpoons HF(v+1) + H_2(v'-1)$$

Preceding page blank

-11-
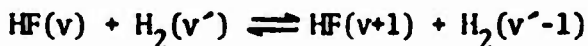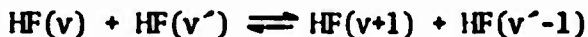
5. Dissociation-recombination

$$F_2 + M \rightleftharpoons M + F + F$$

$$H_2 + M \rightleftharpoons M + H + H$$

$$HF(v) + M \rightleftharpoons M + H + F$$
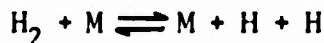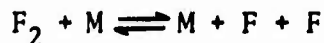
This reaction system is approximated by the 79 reactions and rate coefficients listed in the Appendix. Except as noted, the rate coefficients are those suggested by Cohen.[20]

Photolytic initiation, i.e., dissociation of F_2 by the flashlamp, is modeled by the F-atom production rate

$$\frac{dN_F}{dt} = 2Z_1 I(t) \left[1 - \exp(-Z_2 N_{F_2}) \right] \tag{1}$$

where $I(t)$ is the flash intensity normalized to have a maximum of unity, Z_1 is the maximum output of the lamp in moles of photons per unit laser volume per sec, and Z_2 is the product of a mean absorption coefficient and absorption length.

The chemical reactions are written as

$$\sum_i \alpha_{ri} N_i \underset{k_{-r}}{\overset{k_r}{\rightleftharpoons}} \sum_i \beta_{ri} N_i \tag{2}$$

where N_i is the molar concentration of species i, α_{ri} and β_{ri} are stoichiometric coefficients, and k_r and k_{-r} are forward and backward rate coefficients.

The rate of change of concentration $N(v)$ for vibrational level v is given by

$$\frac{dN(v)}{dt} = X_{rad}(v,J) - X_{rad}(v-1,J_L) + X_{ch}(v) \tag{3}$$

where $X_{rad}(v,J)$ is the rate of change of concentration resulting from lasing from $v + 1$ to v. Lower level rotational quantum numbers J and J_L are selected as those giving maximum gain for transitions $v + 1 \rightarrow v$ and $v \rightarrow v - 1$, respectively. The rate of change of $N(v)$ resulting from chemical reactions $X_{ch}(v)$ is

$$X_{ch}(v) = \sum_r (\beta_{ri} - \alpha_{ri}) L_r \tag{4}$$

where

$$L_r = k_r \prod_j N_j^{\alpha_{rj}} - k_{-r} \prod_j N_j^{\beta_{rj}}$$

The laser cavity is assumed to have a uniform photon flux with active medium length L and mirror reflectivities R_0 and R_L. Lasing initiates for any $v + 1 \rightarrow v$ band when the gain for the highest gain transition of that band is equal to the threshold gain α_{thr}, where

$$\alpha_{thr} = -\frac{1}{2L} \ln(R_0 R_L) \tag{5}$$

The gain is assumed constant over length L. As only P-branch transitions need be considered, the gain of a transition with lower level v, J is

$$\alpha(v,J) = \frac{h N_A}{4\pi} \omega_C(v,J) \phi(v,J) B(v,J) \left[\frac{2J + 1}{2J - 1} N(v + 1, J - 1) - N(v,J) \right] \tag{6}$$

The wave number of the transition is $\omega_C(v,J)$, $B(v,J)$ is the Einstein isotropic absorption coefficient based on the intensity, and N_A is Avogadro's number. Line-broadening constants and resonance constants used in the Voigt profile at line center $\phi(v,J)$ are those of Ref. 19.

The Boltzmann distribution of the rotational populations is given by

$$N(v,J) = N(v) \frac{(2J + 1)}{Q_r^V (T)} \exp \left[-hcE_J^V/kT \right] \qquad (7)$$

where values of the rotational partition function $Q_r^V (T)$ and rotational energy E_J^V are from the data of Mann, et al.[25] Planck's constant, the speed of light, and Boltzmann's constant are denoted as h, c, and k, respectively. The energy equation for a constant density gas is written in the form

$$\sum_i N_i C_{p_i} \frac{dT}{dt} - \frac{dp}{dt} = - P_L - \sum_i \frac{dN_i}{dt} H_i \qquad (8)$$

where C_{p_i} is the specific heat at constant pressure and H_i is the molar enthalpy of species i, p is the pressure, and P_L is the output lasing power per unit volume. The power is

$$P_L(t) = \sum_{v=0}^{5} hcN_A \omega_c (v,J) X_{rad} (v,J) \qquad (9)$$

Numerical integration of Eqs. (1), (3), (8), and the equation of state determines the pressure, temperature, and species concentrations until, at some time t_0 and for some value $J = J_0$, the gain on a given vibration-rotation transition reaches α_{thr}. At this time, the laser pulse begins. Then Eqs. (1), (3), (5), (8) and the equation of state are solved for the transient temperature, pressure, concentrations, and, for each band that is lasing, output power and active J. During lasing, this value of J shifts sequentially to larger values because of HF concentration growth and temperature rise. Lasing terminates when all $\alpha(v,J)$ become less than α_{thr}.

The laser power $P_L(t)$ in Eq. (8) is the sum from both mirrors of the cavity. The power extracted from mirror R_0 is

$$P_0 = \frac{(1 - R_0)}{[1 + (R_0/R_L)^{1/2}][1 - (R_0 R_L)^{1/2}]} P_L(t) \tag{10}$$

Initial conditions and model parameters are determined to reflect conditions of the experiments. In these experiments, the laser has an active medium length of 53.3 cm. The optical cavity is formed by a gold-coated mirror, with nominal reflectivity of 0.98, and one of two partially transmitting mirrors — a 25% transmitting dielectric-coated sapphire flat or a 65% transmitting ar-coated silicon flat. Other losses in the cavity were lumped with the 98% reflecting gold mirror for an estimated value $R_L = 0.9$. The output mirrors were taken as $R_0 = 0.75$ and 0.35, respectively. Initial concentrations were matched to those of the experiment, including the effect of prereaction (Fig. 1). The normalized flashlamp profile was determined (Fig. 2) and taken as $I(t)$. At these low concentrations, the mixture is optically thin, i.e., $Z_2 N_{F_2} \ll 1$; hence, Eq. (1) becomes

$$\frac{dN_F}{dt} \cong 2 Z_1 Z_2 I(t) N_{F_2} \tag{11}$$

Therefore, only the product $Z_1 Z_2$ is necessary to model the flashlamp coupling. Because an independent measure of $Z_1 Z_2$ was not available, we determine this parameter to be $2.1 \times 10^3 \text{sec}^{-1}$ by matching the computed time for the laser
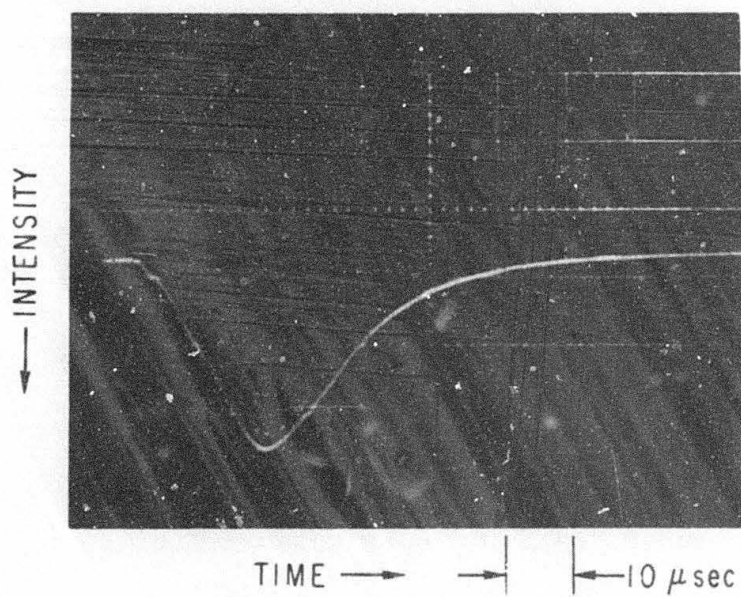
Fig. 2. Flashlamp Intensity vs Time Observed
Through a 290 ± 10 nm Spectral Filter

to reach threshold to the measured time for the case $H_2:F_2:HE = 0.1:1:20$ with the 25% transmitting output mirror. This procedure seemed most satisfactory, as time-to-threshold predictions for this case depend on only a few parameters (Z_1Z_2, pumping rates, and α_{thr}).

IV. RESULTS AND DISCUSSION

In the sections that follow, the results of our experimental and theoretical investigations are compared. Interpretation of the character of the laser pulse is given in regions where experiment and theory agree. In regions of disagreement, the probable cause for deviation of experiment and theory is isolated and additional experimental results are presented to enhance the interpretation of the disagreement.

A. PULSE SHAPE

Experimental intensity vs time records are found to exhibit three types of pulse shape. Pulses for very low H_2 have peak intensity at the beginning and then an irregular decay to zero. Additionally, these records have pronounced transients superposed on the basic pulse shape. Pulses for experiments with somewhat larger H_2 rise from threshold to peak intensity in several distinct steps. After peak intensity, there is a smooth decay to zero. Additional transients are less pronounced in these records. Finally, for H_2 near stoichiometric, the pulses have small initial steps and a smooth rise to peak intensity and decay to zero. Records of the observed pulse shapes with the 25% output coupler for $F_2/He = 1/20$ and $1/40$ are presented in Fig. 3. Also shown in this figure are predicted intensity vs time pulse shapes. In order to facilitate comparison, the intensity scale for each computed pulse is selected so that the peak intensity is approximately the same fraction of the ordinate as the observed pulse; the time scales are identical. Except for the transients in the experiment, the main features of these pulse shapes are predicted quite well by

Preceding page blank
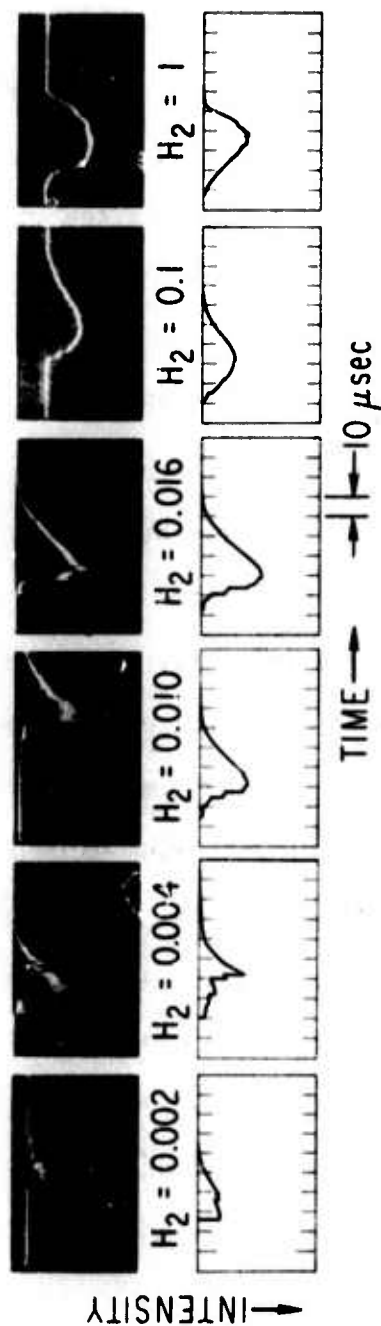
(a) $F_2/He = 1/40$, 25% OUTPUT COUPLER; UPPER ROW EXPERIMENTAL, LOWER ROW COMPUTER PREDICTION
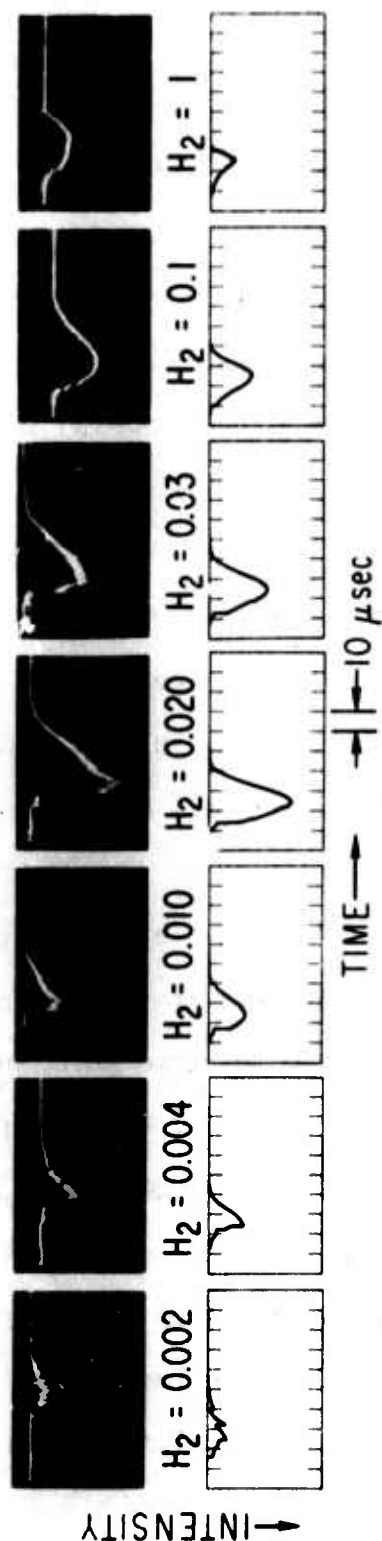
(b) $F_2/He = 1/20$, 25% OUTPUT COUPLER; UPPER ROW EXPERIMENTAL, LOWER ROW COMPUTER PREDICTION

Fig. 3. Observed and Predicted Effect of H_2 on Intensity and Pulse Shape for $H_2 + F_2$ Chain Reaction Laser

the theoretical model. The time location of the observed laser pulses is somewhat arbitrary because, in some cases, flashlamp triggering was delayed relative to oscilloscope triggering. In the next sections we find that, when these triggering problems were averted, the observed and predicted time locations were in good agreement.

With the knowledge that observed and predicted pulse shapes are similar, we selected three pulse characteristics for quantitative comparison. These are: time from onset of the flashlamp until laser threshold, pulse duration measured from laser threshold to the point in the tail of the pulse where the intensity has fallen to one-tenth its peak value, and the peak intensity during the pulse. For brevity, we refer to these parameters as: time to threshold, pulse duration, and peak intensity.

B. TIME TO THRESHOLD

Observed and predicted values of time to threshold for $F_2/He = 1/20$ and for both output couplers are in good agreement as seen in Fig. 4. As expected, the time required to reach threshold increases as the initial H_2 decreases. For small H_2, threshold is not achieved. Synchronization difficulties caused erratic time-to-threshold data for the $F_2/He = 1/40$ mixtures; however, results similar to those in Fig. 4 were found for these mixtures in earlier experiments.

Chester and Hess[26] compared theoretical and experimental values of time to threshold for a pulsed HF laser based on flash photolysis of $MoF_6 + H_2$ mixtures. They found good agreement over a range of mixture pressures. Detailed prediction of other features of the laser pulses was not included within the scope of their study.
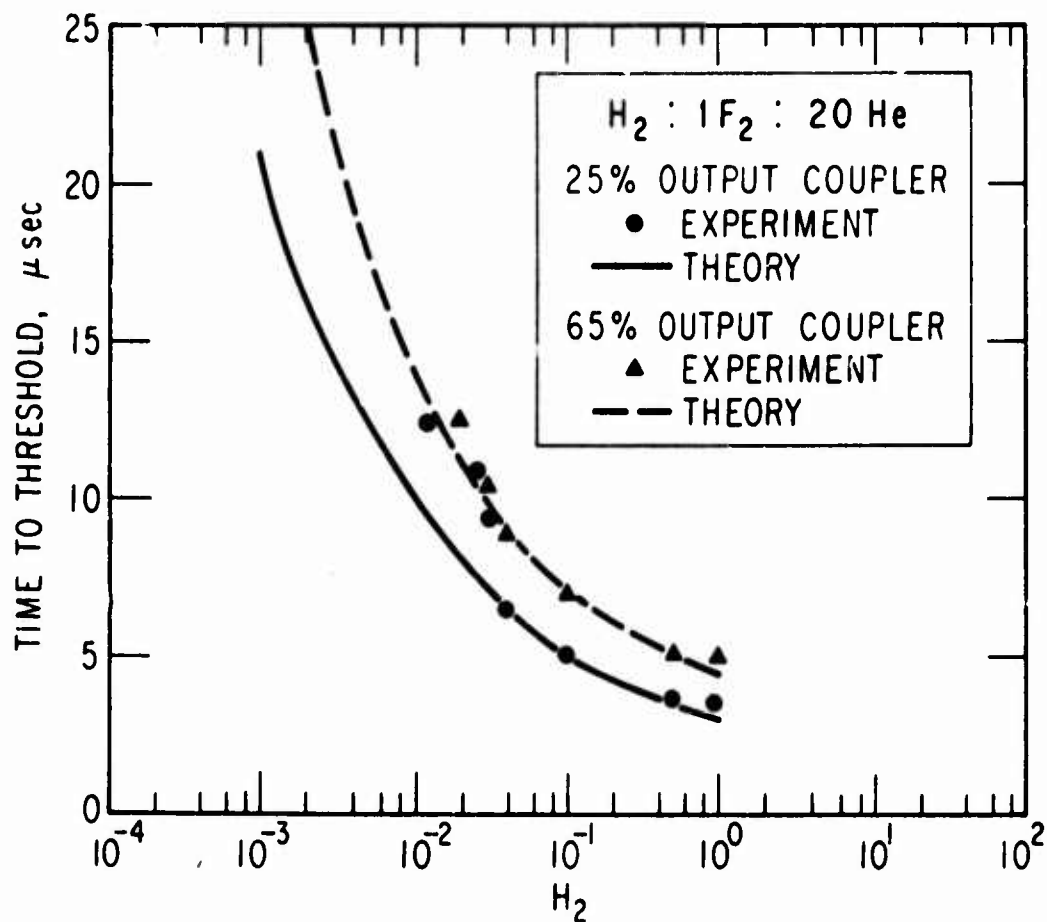
Fig. 4. Observed and Predicted Time to Achieve Laser Threshold as a Function of H_2 for Initial Composition Ratio $H_2:F_2:He = H_2:1:20$ and for 25 and 65% Transmitting Output Mirrors

C. PULSE DURATION

In Fig. 5, observed and predicted pulse durations are compared as a function of H_2 for the four cases studied. The overall agreement is good. For $H_2:F_2:He = H_2:1:40$ and the 25% output mirror, there is excellent agreement. The main trends are the same for the other cases, but there are some deviations between theory and experiment. For example, the theoretical point in Fig. 5d that is quite high stems from a condition that produced an output with a double spike; the small second spike results when, in the calculation, the gain on another vibrational transition achieves threshold. The pulse duration of the first spike at this same concentration is in good agreement with experiment.

An upper limit on the laser pulse duration is imposed by the time required to consume the H_2, i.e., the reaction duration. The reaction duration is nearly constant for small H_2 where the heat release is negligible. For increasing H_2 above $H_2/F_2 = 0.1$, however, there is a decreasing trend to the reaction duration caused by thermal acceleration of the pumping rates. This decreasing trend appears for both experiment and theory in all four cases of Fig. 5.

The laser pulse is actually shorter than the reaction duration. A finite time interval of pumping occurs before lasing begins, and deactivation processes quench the laser before the reaction is complete. In the model, the dominant deactivators are F (Reacts. 44-50), H (Reacts. 23-29), and HF (Reacts. 37-43); their relative importance depends on the initial H_2/F_2 ratio. For $H_2/F_2 < 0.01$, deactivation by F dominates. For $H_2/F_2 > 0.01$, deactivation by HF and H is more important.

As H_2 is increased, a "knee" is found in the theoretical prediction of pulse duration and is most evident for the $F_2/He = 1/40$ mixture with the 65%
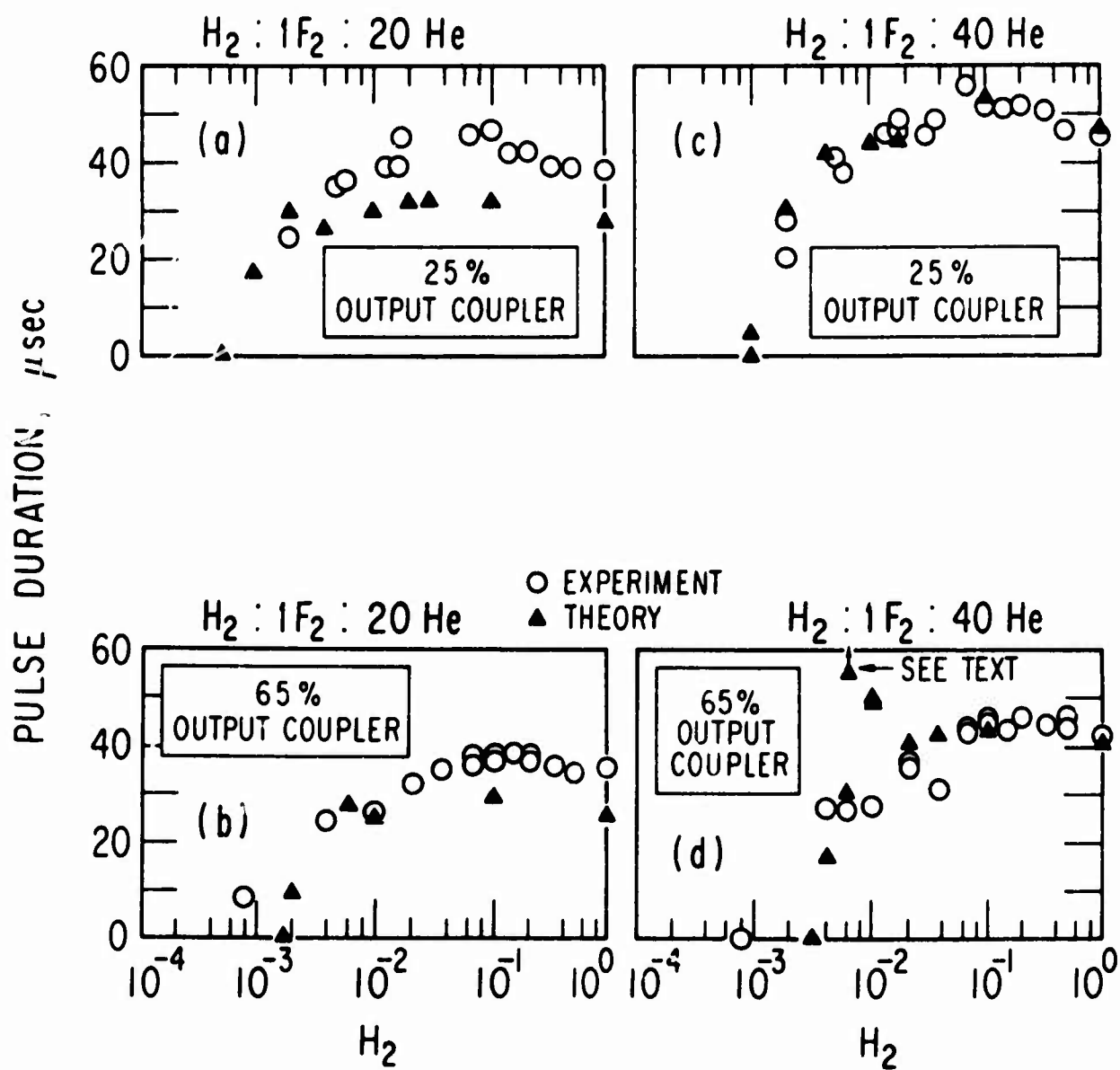
-23-

Fig. 5. Observed and Predicted Pulse Duration vs Parts H_2

output coupler. This "knee" occurs where the computation changes abruptly from predomination of lasing on bands associated with the pumping reactions $F + H_2$ (Reacts. 11-13) to lasing on all bands associated with the chain and, hence, a much higher degree of cascading. This abrupt behavior was not observed experimentally.

The following section presents evidence that leads us to the conclusion that parasitic oscillations rob power from the observed laser beam, especially in the regime $H_2/F_2 > 0.1$. Based on the good agreement shown in Figs. 4 and 5, it appears that time to threshold and pulse duration are little affected by these parasitics. This is in marked contrast to the behavior of some ruby lasers where the onset of parasitic oscillations causes premature quenching of the observed laser beam[27] or of some glass lasers where parasitics reach threshold first and quench the observed beam altogether.[28]

D. PEAK INTENSITY

In Fig. 6 are presented the theoretical curves and experimental data for peak intensity vs parts H_2 for the four cases studied. In interpreting the experimental records, an average is used when transients occur in the vicinity of the peak intensity. These plots show that, below one-tenth part H_2, theory and experiment have the same trends. Above this H_2 pressure, the agreement vanishes; theoretical peak intensity continues to increase with H_2, while the experiments exhibit an abrupt leveling off. The best agreement is observed in Figs. 6c and 6d and the poorest agreement in Figs. 6a and 6b. For a fixed H_2/F_2 ratio, the small-signal gain is lower for mixtures represented in Figs. 6c and 6d than those in Figs. 6a and 6b as shown in Fig. 7. The influence of gain on these observations will be discussed again shortly.
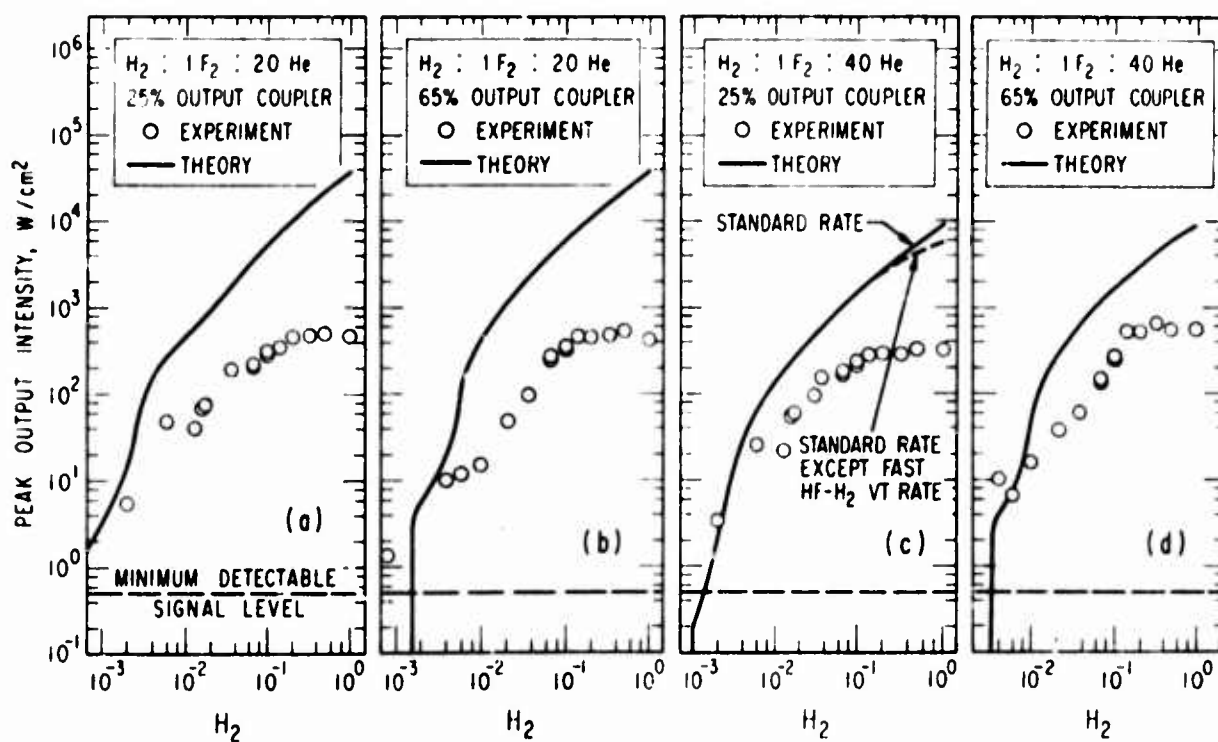
Fig. 6. Observed and Predicted Intensity vs H_2

(a)

R_W

$R_W = 0.1$
$L = 1.1$ cm

$(R_W)^3 e^{3gL} = 1 \Rightarrow g = 2.09$ cm^{-1}

(b)

R_L R_W R_O

$R_L = 0.90$
$R_O = 0.35$
$R_W = 0.95$
$L = 53.3$ cm

$R_L R_O (R_W)^2 e^{2gL} = 1 \Rightarrow g = 0.0118$ cm^{-1}

PARASITIC (a)

PARASITIC (b)

1/20 - F_2/He
1/40 - F_2/He

65 % OUTPUT COUPLER

25 % OUTPUT COUPLER

MAXIMUM SMALL SIGNAL GAIN, α (cm^{-1})

10^1
10^0
10^{-1}
10^{-2}
10^{-3}

10^{-4} 10^{-3} 10^{-2} 10^{-1} 10^0

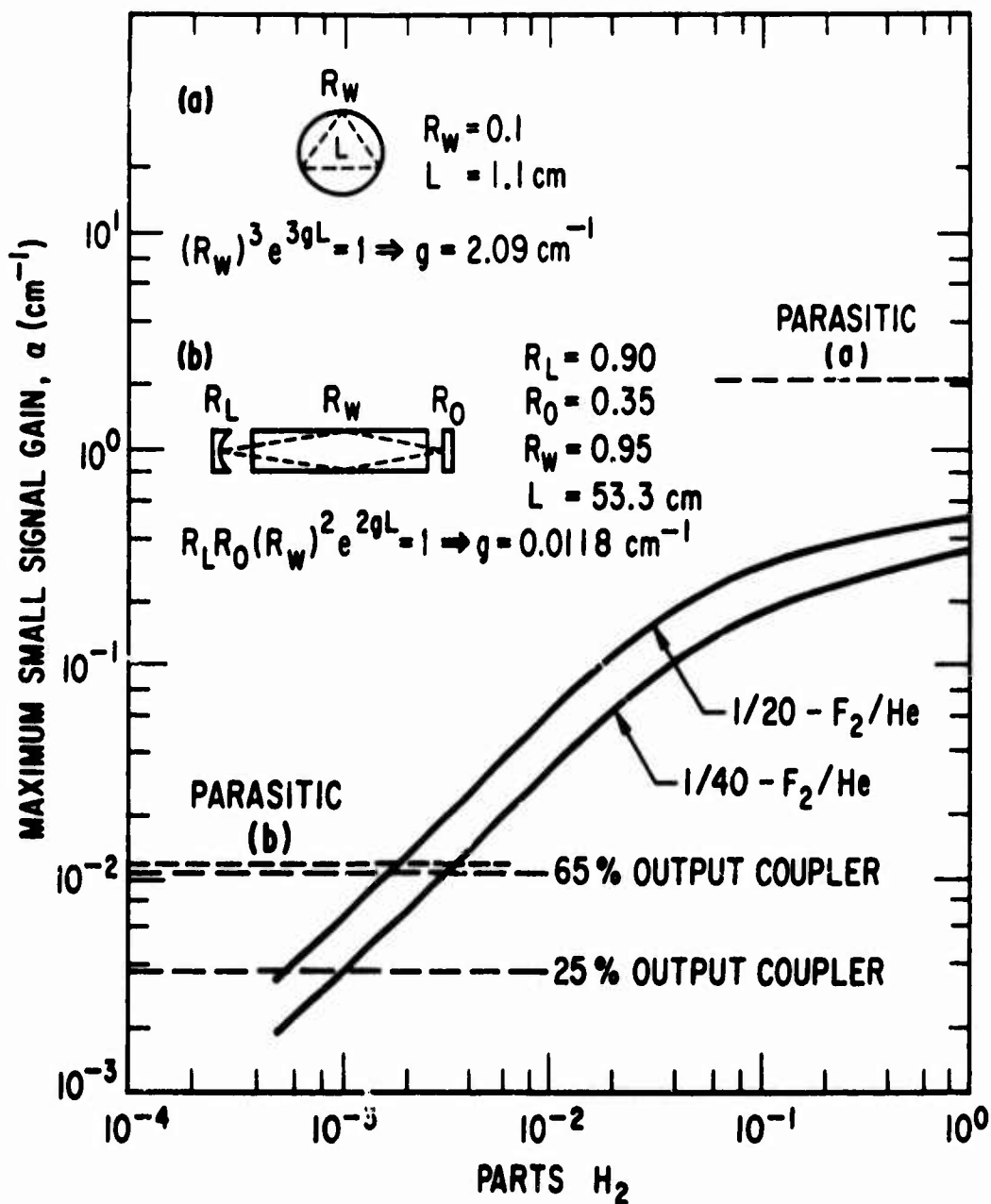PARTS H$_2$

Fig. 7. Predicted Values of Maximum Small Signal Gain vs H$_2$ for Mixtures with Initial Composition Ratio H$_2^2$:F:He = H$_2$:1:20 and H$_2$:1:40

A similar, but more severe, experimental trend is reported by Hess[11] for cases with a composition ratio $H_2:F_2:He = H_2:1:40$, pressures near 160 Torr, and a 99-cm laser tube. His data show that, on increasing the H_2/F_2 ratio from 0.33 to 1.0, the observed peak power decreases by nearly a factor of three.

The discrepancy shown in Fig. 6 is investigated by an evaluation of the effect of uncertainties in rate coefficients for the deactivation mechanisms. As a limiting case, we examine the effect of an extreme change in the rate for VT deactivation of HF by H_2 (Reacts. 30-36). In place of the rate coefficient given in the Appendix, which is based on experimental data, we hypothesized a largest plausible rate. This rate was chosen as three times the HF - HF VT rate (see Reacts. 37-43). As shown by the dashed curve in Fig. 6e, this hypothetical fast deactivation causes a moderate reduction in the predicted peak intensities for the larger values of H_2. The fast deactivation effect is not large enough to account for the experimental results. Moreover, it occurs gradually; whereas, the experiments show an abrupt leveling off of the peak intensity.

Other variations in rate coefficients were considered. It was known[17] that variations in the pumping reaction rates, pumping reaction distribution, or in the HF - HF and HF - H_2 VV rates within reasonable bounds were not capable of predicting the behavior indicated by the experimental results in Fig. 6. The effect of variations in the HF - F and HF - H VT rate coefficients was also examined. Multiquantum deactivation by these atoms or increases in their efficiency by a factor of 10 also would not account for the observed behavior. In addition, even though the stoichiometric

mixtures for $F_2/He = 1/40$ and $1/20$ reach temperatures as high as 870°K
and 1230°K, respectively, at pulse termination, the uncertainty in
the temperature dependence of the major mechanisms is not sufficient to
explain the experimental results.[17,20] These uncertainties in the
kinetics showed less pronounced effects than that illustrated by the
dashed curve in Fig. 6c. We therefore conclude that it is improbable
that a purely kinetic explanation exists for the leveling off of
experimental peak intensity shown in Fig. 6.

Explanations for the sharp leveling off of peak intensity may also
be sought in the area of undesired optical phenomena. The actual laser
is more complicated than assumed in the theory and is subject to
several problems. Spatial nonuniformity of the reaction and concomitant
gradients of refractive index may increase cavity losses, as well as
steer the beam away from the detector. A host of parasitic lasing modes
is also conceivable because of the high gain of the medium and because
the reaction occurs within a tube whose wall and windows are not
perfectly transmitting. Because parasitic oscillations are known to
occur in solid-state lasers under high-gain conditions,[28-30] we have
given them first attention.

Parasitic modes are those that reflect off the tube's wall and are
regenerative. We will limit our discussion to two possible types:
circumferential or whispering modes and axial modes. Nonparasitic modes
are referred to as fundamental (either longitudinal or transverse)
modes.

The likelihood of parasitic modes is shown in Fig. 7 by an order of magnitude comparison between the largest small-signal gain of the medium and the gains required for threshold for several modes of oscillation in our apparatus. Threshold gains for wall grazing modes with either near-axial or circumferential paths are obtained by use of expressions including Fresnel law estimates of losses suffered in near-grazing reflections at the laser tube wall (Fig. 7). In making these threshold estimates, we neglect gain saturation due to competing modes. Likewise, we do not account for mode-coupling effects that could cause a lowering of the threshold gain for certain parasitic modes.[31,32]

Figure 7 shows that variation of the H_2 pressure serves as a convenient way of varying the peak small-signal gain over several orders of magnitude. As expected, peak gains are larger for the less dilute mixture. As H_2 increases, the small-signal gain for either mixture becomes nearly as large as the threshold for circumferential modes and much larger than the threshold values for either fundamental or near-axial grazing modes. The fundamental modes of lowest loss saturate the gain down the center of the laser tube but not near its walls. A competition for this outer annulus of high gain exists between fundamental modes with greater losses (i.e., high-order transverse modes) and near-axial grazing modes, either of which can degrade the intensity along the laser axis. Grazing modes, once oscillating, are particularly detrimental to our comparison (Fig. 6), because they extract energy when passing near the tube center that might otherwise be emitted in a longitudinal mode that contributes to the measured intensity.[28,29]

Measurements of the output intensity of flash photolysis $UF_6 + H_2$ and $MoF_6 + H_2$ lasers as a function of the total sample pressure by Dolgov-Savel'yev[7] have shown a similar behavior. As the sample pressure was increased, the laser output intensity for the $MoF_6 + H_2$ mixture was found to first increase with pressure, then decrease with further increasing sample pressure. Similar results were found in the $UF_6 + H_2$ system. These observations can also be explained in terms of parasitic oscillations. This is because an increase in sample pressure corresponds to an increase in the gain of the system if we assume that their samples are optically thin to the flashlamp radiation and that Doppler broadening is controlling the gain. Once the system gain has reached a critical value, a further increase in sample pressure will lead to the onset of parasitic oscillations and a decrease in the fundamental mode laser intensity.

Supplementary experimental results are given that serve to isolate further the nature of the discrepancies in Fig. 6. In one set of experiments, total small-signal gain is varied by a change in the length of the active medium. In another, the effect on laser spot size of gain coefficient variation is studied. Both experiments lend credence to the idea that nonideal optical behavior is present.

Previous studies[33] indicate that parasitic oscillations are difficult to avoid when the total small-signal gain exceeds a critical value. Thus, experiments that vary this gain by changing the length of active medium are expected to be informative. Such experiments are performed by the

use of masks outside the laser tube to change the length of the photolyzed medium. Measurements are made of peak intensity as a function of the H_2 pressure with illuminated lengths of 10, 5, and 2.5 cm, with a laser mixture of $F_2/He = 1/20$ and 25% output coupling. The results of these measurements are shown in Fig. 8. In the 10-cm case, the trends are much the same as with the 53.3-cm length. With the 5-cm active length, intensity leveled off at 1/10 part H_2, but no decrease in power was observed on further increasing the H_2. Data for the 2.5-cm active length agree more closely with the theoretical trend, because they exhibit a monotonic increase. Also displayed in Fig. 8 are the results of Hess.[11]* The trend observed in this laser peak intensity agrees well with the pattern of trends we observed.

The effect of decreasing the length is reflected in the theoretical model through Eqs. (5) and (10). For mixtures capable of attaining gains well above threshold, the variation of peak intensity with length is dominated by Eq. (10). Therefore, the model implies that the peak intensity should vary proportional to L for $H_2 \gtrsim 1/100$ part. This trend is shown by the data in Fig. 8.

With an active laser length of 2.5 cm, a moderate leveling off of the peak HF power was observed. A possible explanation for this effect, the threshold estimates of Fig. 7 notwithstanding, may be the existence of circumferential modes. These modes can oscillate independent of the laser length, as they are dependent only on the gain and the reflection angle from

---

*We have converted the power data of Ref. 15 to intensity by dividing by a detector area of 0.0314 cm^2.[34]
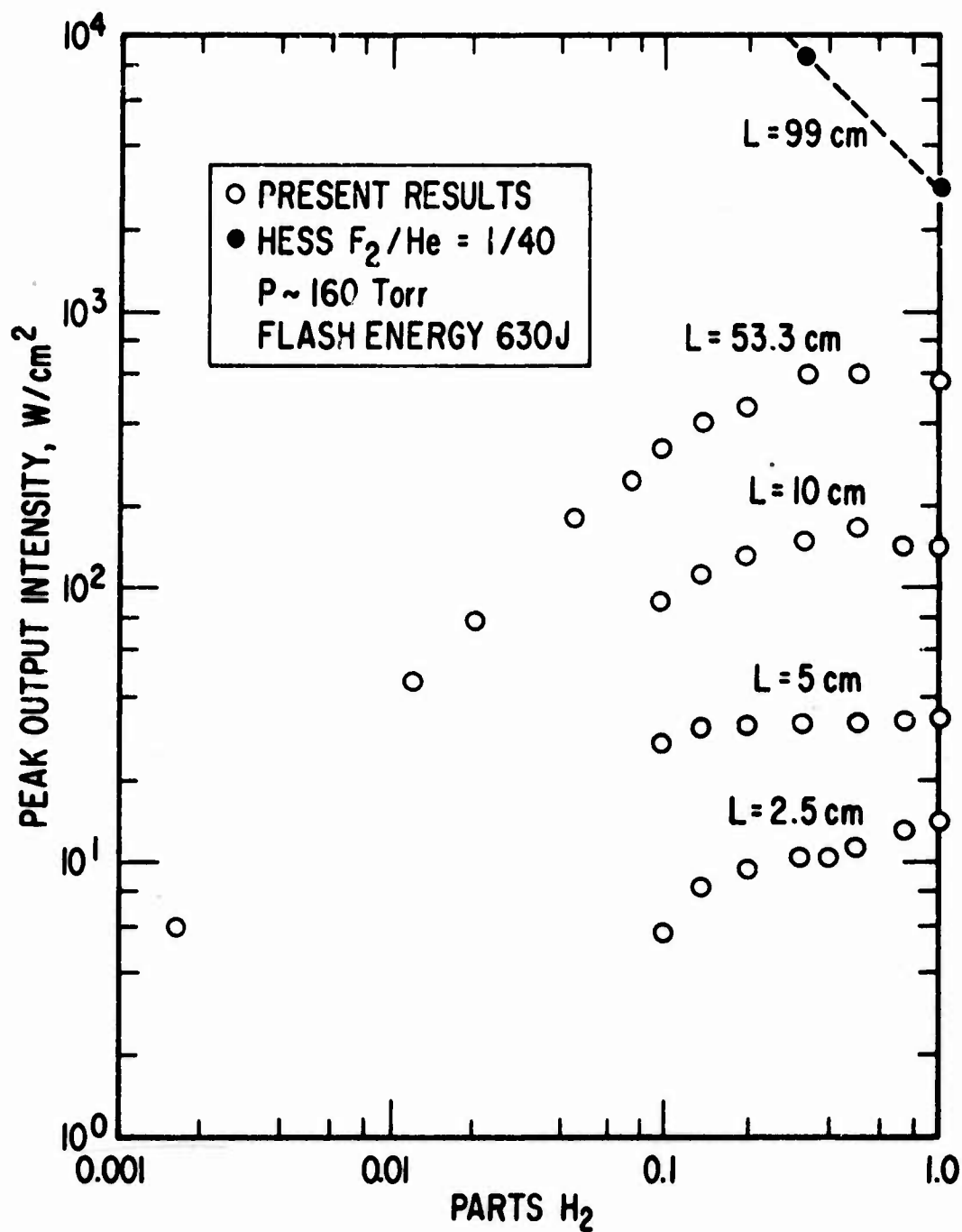
Fig. 8. Effect of Laser Tube Length Exposed to Photolysis
on Observations of Peak Intensity vs H_2

-33-

the inner surface of the laser tube. Whispering laser modes have previously been observed in a Sm^{++} doped CaF_2 sphere of radius 1 mm and solid-state toroids.[35,36]

In a second set of experiments, the effect of gain variation on laser spot size was studied. We define the laser spot size as the largest diameter of an iris, external to the laser cavity, through which the laser beam passes with uniform intensity, i.e., beam power varies as the square of the radius. As the flashlamp energy increases, the fraction of F_2 molecules dissociated to F atoms increases. Consequently, increasing flashlamp energy increases the rate at which the $H_2 + F_2$ chain runs, and this increases the small-signal gain. It was found that, as the flash energy increased from zero, the laser spot size increased in diameter. A further increase in energy did not effect the spot size, and finally, at high flash energies, the spot size was found to vary inversely with flash energy. The increase in spot size at low flash energies can be explained by an increase in the number of fundamental laser modes that reach threshold as the flash energy increases. We expect parasitic oscillations to compete with these modes, however, and ultimately cause the spot to decrease.

V. CONCLUSIONS

Stimulated emission from an HF chemical laser is shown to be well predicted by a theoretical model that is based on chemical rate equations and that assumes constant gain and rotational equilibrium. For an $H_2 + F_2$ chain reaction laser initiated by flash photolysis, comparisons of pulse shape, time to threshold, pulse duration, and peak intensity show excellent agreement considering the approximations of the model. Where cavity transients are observable, the constant gain predictions agree with a smoothed curve through the average of the transients.

Detailed study of the effect of H_2 partial pressure on laser performance is a useful diagnostic technique for identifying the presence of undesired optical behavior. With this technique, we have shown the regime $H_2/F_2 > 0.1$ as one where parasitic oscillations are believed to occur and to dominate the interpretation of the experiment. Supplementary calculations and experiments tend to confirm this. Spatially-resolved laser output measurements are needed to delineate further the character of parasitics. On the basis of these results, we are led to the conclusion that previous pulsed $H_2 + F_2$ laser investigations may, in part, show misleadingly small laser outputs because of parasitic oscillations.

VI. REFERENCES

1.   N. G. Basov, L. V. Kulokov, Ye. P. Markin, A. I. Nikitin, and A. N. Oraevsky, _JETP Lett._ **9**, 375 (1969).

2.   O. M. Batovskii, G. K. Vasil'ev, E. F. Makarov, and V. L. Tal'rose, _JETP Lett._ **9**, 200 (1969).

3.   O. M. Batovskii, G. K. Vasil'ev, and V. L. Tal'rose, _International Symposium on Chemical Lasers_, Sept. 1969, Moscow.

4.   V. S. Burmasr, G. G. Dolgov-Savel'yev, V. A. Polyakov, and G. M. Chumak, _JETP Lett._ **10**, 28 (1969).

5.   G. M. Chumak, G. G. Dolgov-Savel'yev, and V. A. Polyakov, _International Symposium on Chemical Lasers_, Sept. 1969, Moscow.

6.   N. G. Basov, E. P. Markin, A. I. Nikitin, and A. N. Oraevsky, _IEEE J. Quant. Elect._ QE-6, 183 (1970).

7.   G. G. Dolgov-Savel'yev, V. A. Polyakov, and G. M. Chumak, _JETP_ **31**, 643 (1970).

8.   N. G. Basov, V. T. Galochkin, V. I. Igoshin, L. V. Kulakov, E. P. Markin, A. I. Nikitin, and A. N. Oraevsky, _Appl. Opt._ **10**, 1814 (1971).

9.   N. G. Basov, V. I. Igoshin, E. P. Markin, and A. N. Oraevsky, _Kvantovaja Electronika_ **2**, 3 (1971).

10. L. D. Hess, _Appl. Phys. Letters_ **19**, 1 (1971).

Preceding page blank

11. L. D. Hess, J. Chem. Phys. 55, 2466 (1971).

12. S. N. Suchard, R. W. F. Gross, and J. G. Whittier, Appl. Phys. Letters 19, 411 (1971).

13. G. G. Dolgov-Savel'yev, V. F. Zharov, Yu. S. Neganov, and G. M. Chumak, JETP, 34 34(1972).

14. J. Wilson and J. Stephenson, Appl. Phys. Letters 20, 64(1972).

15. L. D. Hess, J. Appl. Phys., 43, 1157(1972).

16. J. Wilson, D. Northam, and P. Lewis, Paper presented at Third Conference on Chemical and Molecular Lasers, St. Louis, Mo., May 1972.

17. R. L. Kerber, G. Emanuel, and J. S. Whittier, "Computer Modeling and Parametric Study for a Pulsed H_2 + F_2 Laser," Applied Optics 11, 1112 (1972).

18. J. R. Airey, J. Chem. Phys. 52, 156 (1970).

19. G. Emanuel, W. D. Adams, and E. B. Turner, PISALE - 1: A Chemical Laser Computer Program, Technical Report TR-0172(2776)-1, The Aerospace Corporation, El Segundo, California (15 Mar 1972).

20. N. Cohen, A Review of Rate Coefficients for Reactions in the H_2 - F_2 Laser System, Technical Report TR-0172(2779)-2, The Aerospace Corporation, El Segundo, California (3 Sept 1971).

21. A. V. Grosse and A. D. Kirshenbaum, J. Phys. Soc. Japan 77, 5012, (1955).

22. R. K. Steunenberg and R. C. Vogel, J. Am. Chem. Soc. 78, 901 (1956).

23. S. N. Suchard and L. D. Bergeson (to be published in Rev. Sci. Instr.).

24. M. C. Lin and W. H. Green, J. Chem. Phys. 53, 3383 (1970).

25. D. E. Mann, B. A. Thrush, D. R. Lide, J. J. Ball, and N. A. Acquista, J. Chem. Phys. 34, 420 (1961).

26. A. Chester and L. D. Hess, IEEE J. Quantum Electronics, QE-8, 1 (1972).

27. A. E. Siegman and J. W. Allen, IEEE J. Quantum Electronics, QE-1, 386 (1965).

28. D. Röss and P. Mockel, Z. Naturforsch 20a, 49 (1965).

29. D. Röss, Z. Naturforsch 20a, 264 (1965).

30. W. R. Sooy, R. S. Congleton, B. E. Dobratz, and W. K. Ng, Proc. Third Intl. Congress on Quant. Electronics, Vol. 2, ed. P. Grivet and N. Bloembergen, Columbia University Press, New York (1964).

31. R. J. Collins and J. A. Giordmaine, Proc. Third Intl. Congress on Quant. Electronics, ed. P. Grivet and N. Bloembergen, Columbia University Press, New York (1964), pp. 1239-1246.

32. C. M. Varma, IEEE J. Quantum Electronics, QE-5, 78 (1969).

33. P. A. Miles and J. W. Lotus, IEEE J. Quantum Electronics, QE-4, 811 (1968).

34. L. D. Hess, private communication (1971).

35. C. G. B. Garrett, W. Kaiser, and W. L. Bond, $\underline{\text{Phys. Rev.}}$ $\underline{124}$, 1807 (1961).

36. G. Röss and G. Gehrer, $\underline{\text{Proc. of IEEE}}$, $\underline{52}$, 1359 (1964).

37. P. Wilkins, $\underline{\text{Monte Carlo Calculations of Reaction Rates and Energy Distributions Among Reaction Products, I. F + H}_2 \rightarrow \text{HF + H}}$, Technical Report TR-0172(2776)-4, The Aerospace Corporation, El Segundo, Calif. (April 1972).

38. J. F. Bott and N. Cohen, $\underline{\text{J. Chem. Phys.}}$ $\underline{55}$, 3698 (1971).

39. B. A. Ridley and I. W. M. Smith, $\underline{\text{Chem. Phys. Letters}}$ $\underline{9}$, 457 (1971).

40. D. Rapp and P. Englander-Golden, $\underline{\text{J. Chem. Phys.}}$ $\underline{40}$, 573 (1964).

APPENDIX. THE REACTION SYSTEM

The chemical kinetic model and corresponding rate coefficients used in this study are listed in Table A-I. The rate coefficients are mostly from a compilation prepared by N. Cohen.[20] Several additional studies have appeared recently, however, and the present rates reflect the new data. Implications of the difference in rates between the table and Ref. 20 are not serious and are covered in the footnotes of Table A-I.

Some of the catalytic species listed at the end of Table A-I are multiplied by a constant. This is equivalent to using a rate coefficient whose value is larger by this factor. The thermodynamic data were taken from the JANAF (Joint Army, Navy, Air Force) publication distributed by the Dow Chemical Corporation. The thermodynamic data of excited species, however, were generated at this laboratory.

Reaction No.	Reaction[1]	Rate Coefficient[2,3]	k(300°)[4]
1	$F_2 + M_1 \rightleftharpoons F + F + M_1$	$k_1 = 5.0 \times 10^{13} e^{35.30}$	9.64×10^{-13}
2	$H_2(0) + M_2 \rightleftharpoons H + H + M_2$	$k_{-2} = 10^{18} T^{-1.0}$	3.33×10^{-15}
3,...,10[5]	$HF(v) + M_1 \rightleftharpoons H + F + M_1$	$k_{3+v} = 1.5 \times 10^{18} T^{-1.0} e^{(135.8-E_v)\theta}$ $v = 0,...,7$	5.93×10^{-84}
11[6]	$F + H_2(0) \rightleftharpoons HF(1) + H$	$k_{11} = 2.7 \times 10^{13} e^{1.60}$	1.84×10^{12}
12	$F + H_2(0) \rightleftharpoons HF(2) + H$	$k_{12} = 3.26 k_{11}$	6.01×10^{12}
13	$F + H_2(0) \rightleftharpoons HF(3) + H$	$k_{13} = 1.63 k_{11}$	3.01×10^{12}
14	$F + H_2(0) \rightleftharpoons HF(4) + H$	$k_{-14} = 4.0 \times 10^{12} T^{0.15} e^{30}$	6.14×10^{10}
15,16	$F + H_2(0) \rightleftharpoons HF(v) + H$	$k_{-10-v} = 1.2 \times 10^{13} T^{0.15}$ $v = 5,6$	2.82×10^{13}
17[6]	$H + F_2 \rightleftharpoons HF(1) + F$	$k_{17} = 6.3 \times 10^{12} e^{2.40}$	1.12×10^{11}
18	$H + F_2 \rightleftharpoons HF(2) + F$	$k_{18} = 1.51 k_{17}$	1.70×10^{11}
19	$H + F_2 \rightleftharpoons HF(3) + F$	$k_{19} = 2.7 k_{17}$	3.03×10^{11}
20	$H + F_2 \rightleftharpoons HF(4) + F$	$k_{20} = 3.33 k_{17}$	3.73×10^{11}
21	$H + F_2 \rightleftharpoons HF(5) + F$	$k_{21} = 5.56 k_{17}$	6.25×10^{11}
22	$H + F_2 \rightleftharpoons HF(6) + F$	$k_{22} = 5.08 k_{17}$	5.71×10^{11}
23,...,29[7]	$HF(v) + M_3 \rightleftharpoons HF(v-1) + M_3$	$k_{22+v} = 6.41 \times 10^1 T^{3.51} e^{-3.940}$ $v = 1,...,7$	2.38×10^{13}
30,...,36[8]	$HF(v) + M_4 \rightleftharpoons HF(v-1) + M_4$	$k_{29+v} = 1.7 \times 10^6 vT^{1.77}$ $v = 1,...,7$	4.12×10^{10}
37,...,43[8]	$HF(v) + M_5 \rightleftharpoons HF(v-1) + M_5$	$k_{36+v} = 1.7 \times 10^6 vT^{1.77} + 1.1 \times 10^{13} vT^{-0.4}$ $v = 1,...,7$	1.16×10^{12}
44[9]	$HF(1) + M_6 \rightleftharpoons HF(0) + M_6$	$k_{44} = 1.5 \times 10^{10} T^{1.0} e^{1.18}$	7.11×10^{11}
45[9]	$HF(2) + M_6 \rightleftharpoons HF(1) + M_6$	$k_{45} = 1.5 \times 10^{10} T^{1.0} e^{0.48}$	2.30×10^{12}
46,...,50[9]	$HF(v) + M_6 \rightleftharpoons HF(v-1) + M_6$	$k_{43+v} = 1.5 \times 10^{10} T^{1.0}$ $v = 3,...,7$	4.50×10^{12}
51,...,57[10]	$HF(v) + M_7 \rightleftharpoons HF(v-1) + M_7$	$k_{50+v} = 8.0 \times 10^{-4} vT^{4.0}$ $v = 1,...,7$	6.48×10^6
58,...,63	$2HF(v) \rightleftharpoons HF(v-1) + HF(v+1)$	$k_{57+v} = 1.0 \times 10^8 v(v+1)T^{1.5}$ $v = 1,...,6$	1.04×10^{12}
64,...,68	$HF(v) + HF(v+1) \rightleftharpoons HF(v-1) + HF(v+2)$	$k_{63+v} = 5.0 \times 10^7 v(v+2)T^{1.5}$ $v = 1,...,5$	7.79×10^{11}
69,...,72	$HF(v) + HF(v+2) \rightleftharpoons HF(v-1) + HF(v+3)$	$k_{68+v} = 2.0 \times 10^7 v(v+3)T^{1.5}$ $v = 1,...,4$	4.16×10^{11}
73[11]	$HF(1) + H_2(0) \rightleftharpoons HF(0) + H_2(1)$	$k_{-73} = 2.5 \times 10^8 T^{1.5}$	1.30×10^{12}
74[11]	$HF(2) + H_2(0) \rightleftharpoons HF(1) + H_2(1)$	$k_{-74} = 2.0 \times 10^8 T^{1.5}$	1.04×10^{12}
75[11]	$HF(3) + H_2(0) \rightleftharpoons HF(2) + H_2(1)$	$k_{-75} = 1.3 \times 10^8 T^{1.5}$	6.75×10^{11}
76[11]	$HF(1) + H_2(1) \rightleftharpoons HF(0) + H_2(2)$	$k_{-76} = 1.2 \times 10^9 T^{1.5}$	6.24×10^{12}
77[11]	$HF(2) + H_2(1) \rightleftharpoons HF(1) + H_2(2)$	$k_{-77} = 1.4 \times 10^9 T^{1.5}$	7.27×10^{12}
78,79	$H_2(v) + M_8 \rightleftharpoons H_2(v-1) + M_8$	$k_{77+v} = 2.5 \times 10^{-4} vT^{4.3}$ $v = 1,2$	1.12×10^7

[1]Catalytic species:

M_1 = all species

$M_2 = \sum\limits_{v=0}^{7} HF(v),\ 2.5 \sum\limits_{v=0}^{2} H_2(v),\ 20H,\ F,\ F_2,\ He$

$M_3 = H$

$M_4 = \sum\limits_{v=0}^{2} H_2(v)$

$M_5 = \sum\limits_{v=0}^{7} HF(v)$

$M_6 = F$

$M_7 = F_2,\ 1.5He$

$M_8 = \sum\limits_{v=0}^{7} HF(v),\ 4 \sum\limits_{v=0}^{2} H_2(v),\ H,\ He,\ F,\ F_2$

[2]Rate coefficients k_+ and k_- designate forward and backward rates, respectively, with units in terms of moles, cm^3, and sec. For each reaction, the missing rate coefficient is determined from the equilibrium constant.

[3]The quantity $\theta = -(10^3/RT)$, where the temperature T is in °K and R is 1.987 cal/mole-°K.

[4]For reactions with more than one value of v, the rate coefficient at 300°K is given for the smallest v.

[5]Vibrational energy above the ground state is denoted as E_v.

[6]Overall pumping of Reactions (11) through (13) and (17) through (22), and their distribution with $v (v \geq 1)$ are the same as Ref. 20; however, based on calculations by Wilkins,[37] these reactions do not populate $v = 0$.

[7]The SSH rate calculated by Cohen[20] is used. This rate is so large that it was assumed independent of v.

[8]Rates of Reactions (37) through (43) are essentially the same as Ref. 20 at 300°K; however, we have used a slightly different temperature variation that reflects an earlier interpretation of the data of Ref. 38. The efficiency of H_2 in deactivating HF(v) is assumed to be the same as HF-HF at high temperatures.

[9]The ratio of $k_{44}:k_{45}:k_{46}$ is assumed to be the same as the rates for deactivation of HCl(v) by Cl, $v = 1, 2, 3$, in Ref. 39. The rate k_{44} is suggested by Cohen[20] for all v; we use k_{46} for $v \geq 3$.

[10]The efficiency of F_2 in deactivating HF(v) is assumed the same as Ar, and the HF(v)-He rate is taken as 1.5 times the Ar rate.[39]

[11]The alternate rate suggested by Cohen[20] based on the Parr and Englander-Golden theory[40] is used after a reevaluation of the experimental data.